INTERNATIONAL JOURNAL FOR NUMERICAL METHODS IN ENGINEERING
Int. J. Numer. Meth. Engng 2008; **73**:185–204
Published online 22 May 2007 in Wiley InterScience (www.interscience.wiley.com). DOI: 10.1002/nme.2068

Computational homogenization for heat conduction in heterogeneous solids

I. Özdemir*,†, W. A. M. Brekelmans and M. G. D. Geers

Department of Mechanical Engineering, Eindhoven University of Technology, P.O. Box 513, 5600 MB Eindhoven, The Netherlands

SUMMARY

In this paper, a multi-scale analysis method for heat transfer in heterogeneous solids is presented. The principles of the method rely on a two-scale computational homogenization approach which is applied successfully for the stress analysis of multi-phase solids under purely mechanical loading. The present paper extends this methodology to heat conduction problems. The flexibility of the method permits one to take into account local microstructural heterogeneities and thermal anisotropy, including non-linearities which might arise at some stage of the thermal loading history. The resulting complex microstructural response is transferred back to the macro level in a consistent manner. A proper macro to micro transition is established in terms of the applied boundary conditions and likewise a micro to macro transition is formulated in the form of consistent averaging relations. Imposition of boundary conditions and extraction of macroscopic quantities are elaborated in detail. A nested finite element solution procedure is outlined, and the effectiveness of the approach is demonstrated by some illustrative example problems. Copyright © 2007 John Wiley & Sons, Ltd.

Received 3 November 2006; Revised 22 January 2007; Accepted 17 March 2007

KEY WORDS: multi-scale; computational homogenization; heat conduction; FE^2; thermomechanics; coarse graining

1. INTRODUCTION

Materials with a high temperature resistance are indispensable in many engineering applications. Refractories used in furnace linings, thermal coatings and microelectronic components are just a few examples indicating the wide range of applications where a structure is exposed to strong temperature changes and cycles. The materials selected for such applications are generally far from being homogeneous due to their multi-phase, porous microstructure. Under severe thermal

*Correspondence to: I. Özdemir, Department of Mechanical Engineering, Eindhoven University of Technology, P.O. Box 513, 5600 MB Eindhoven, The Netherlands.
†E-mail: I.Ozdemir@tue.nl

conditions, it is well documented that the damage mechanism originates from the induced stress gradients, the thermal expansion anisotropy and the non-uniformity and mismatches between the constituents at the meso or micro level [1]. Therefore, an accurate prediction of the deterioration process and failure of such components requires a comprehensive understanding of the temperature distribution at all relevant levels of observation, e.g. at the meso and micro level.

Initial research efforts to analyze the behavior of heterogeneous solids were based on variational principles which resulted in bounds for the effective material properties [2]. The approach has been applied to thermoelasticity problems to derive bounds for the thermal expansion coefficient and was further improved to yield tighter bounds on the effective properties [3, 4]. In order to obtain closed-form expressions for effective properties rather than bounds, analytical models were developed that are mainly based on the solution of the problem of an inclusion in an infinite medium. A concise overview of different approaches in the context of heat conduction problems and a comparative study are presented in [5]. However, the predictions of these analytical and variational approaches are restricted to relatively simple geometries with a simple material response, not yielding accurate results when the contrast between the properties of the constituents is large, or when non-continuous interfaces are present.

Asymptotic homogenization approaches, which were originally developed for the solution of differential equations with periodic coefficients, have been exploited for the determination of the (mechanical) constitutive tensor of composites with a periodic microstructure. The method is based on an asymptotic expansion of the unknown field with respect to a micro-scale length parameter, yielding homogenized properties upon truncation of higher-order terms. Due to its generality, this approach is also applicable to different field problems as for instance heat conduction problems [6], including higher-order models used to capture size effects [7].

The finite element solution of the fine-scale problem considered in an asymptotic homogenization framework, from which the relevant material characteristics were obtained numerically, led to the homogenization approach which is introduced in [8]. The method has been extended for thermomechanics and the heat conduction problem in [9–12]. This solution strategy departs from the asymptotic expansion of the temperature field in addition to the displacement field and ends up with homogenized thermal conductivity and thermal expansion coefficients which in turn are used for the solution of the macroscopic thermomechanical problem [13, 14]. However, the problems considered were restricted to small strain linear thermoelasticity and constant conductivity. Moreover, the steady-state heat conduction problem was the main point of interest whereas for some cases the transient effects are pronounced and non-negligible, e.g. in the case of thermoshock.

Relying on the steady evolution of computational tools, analysis methods which are based on the determination of the response from the underlying physics at the finer scales, according to a so-called multi-scale approach, have become feasible. The basic idea is to construct a link between two scales and investigate the interaction between the microstructure and the resulting macroscopic property by using basic material models at the level of single phases on the microscale. A particularly relevant strategy is the computational homogenization approach [15–21], which can be considered as a variant of a global–local analysis. Essentially, the macroscopic predictions are not based on closed-form constitutive equations but the entire material response is computed numerically at each material point by detailed modeling of the microstructure at the point under consideration.

Due to its high computational cost, some alternatives trying to approximate the problem at the micro level with a reduced number of unknowns have been constructed [22, 23]. A particularly relevant one is presented in [22] in which the microstructure is divided into subcells with an

DOI: 10.1002/nme

assumed order of temperature distribution, in which the unknown coefficients are determined by enforcing the compatibility conditions at the subcell walls. Temperature dependency of conductivity is taken into account. The procedure circumvents the heavy computational work but deviates from the experimental data for some geometrical configurations, e.g. twisted yarns. Microstructural details and accuracy of the temperature field at the micro level are important for failure scenarios which initiate from a micro mechanism, e.g. debonding at a fiber matrix interface [24]. Therefore, detailed microstructural information, which can be incorporated *via* computational homogenization, is essential for reliable material response predictions. Furthermore, novel approximate techniques may be properly assessed by taking the computational homogenization results as a reference.

Almost all material properties depend on temperature. Hence, a comprehensive understanding and modeling of the governing phenomena within a multi-scale formalism requires reliable temperature information at all relevant scales. The goal of the present contribution is to construct a computational homogenization approach for the coupled multi-scale analysis of evolving thermal fields in heterogeneous solids with complex microstructures including temperature- and orientation-dependent conductivities. The proposed framework is based on principles used in the computational homogenization approach for stress analyses as presented in [19] and to the authors' knowledge has not been introduced for thermal problems before. It will be shown that the construction of the framework for heat conduction problems poses some fundamental differences compared to its mechanical counterpart and therefore requires a comprehensive treatment.

The paper is outlined as follows. In the next section, the basic principles and assumptions are introduced. Then the problems are defined at two levels i.e. at macro and at micro scale. Scale transitions are presented in terms of appropriate boundary conditions and the consistency of the bridging structure is shown on the basis of physically motivated principles. The two-scale computation strategy with a nested solution algorithm is briefly described thereafter. Finally, the applicability and the potential of the method is demonstrated on the basis of two example problems followed by some concluding comments.

2. PRELIMINARIES

Computational homogenization is a multi-scale analysis approach in which the material response is obtained from the underlying microstructure by solving a boundary value problem (BVP) defined on a representative volume of the microstructure. Although multiple scales can be embedded within the framework, in this particular case, two distinct levels (scales) are considered which will be referred to as the macro level for the engineering structure and the micro level for the typical fine-scale microstructure of the material under investigation. As will be clarified shortly, there are some basic principles to be taken into account in the definition and distinction of the different scales. First, the fundamental steps of the computational homogenization will be introduced as schematized in Figure 1.

As illustrated in Figure 1, idealization and discretization of an engineering structure toward the solution of a BVP results in a computational model which is used to predict the response, e.g. mechanical or thermal, of the structure under certain loading conditions. To begin with, computational homogenization requires the definition of a microstructural representative volume element (RVE) where characteristic physical and geometrical properties of the fine scale (different phases, internal boundaries, flaws, etc.) are embedded. The scale bridging from macro to micro is achieved by the formulation of consistent boundary conditions in terms of macroscopic quantities

DOI: 10.1002/nme

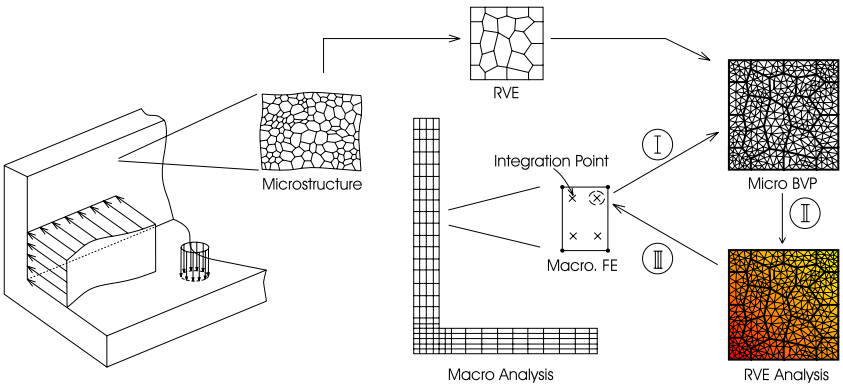

Figure 1. Schematic representation of the computational homogenization scheme.

passed to the micro level (RVE input, shown as step I in Figure 1). Then, the microscopic field excited by the prescribed boundary conditions is resolved by a proper discretization technique applied to the micro-scale BVP (step II in Figure 1). The resulting microscopic quantities are used to extract the macroscopic quantities (step III in Figure 1) *via* a consistent averaging scheme. Furthermore, the linear relation between infinitesimal variations of the RVE output quantities in relation to infinitesimal variations of the input quantities are extracted, i.e. the tangent operator.

In fact, the relevant quantities at both scales involved in the BVP statement are resolved numerically by the finite element method. The scale separation made in such a framework relies on some basic assumptions. The composition of any heterogeneous solid can generally be considered as an assembly of different phases, imperfections, flaws and interfaces. However, as the characteristic dimensions of these microstructural features are still much larger than the molecular dimensions, the use of a continuum approach at this level remains justified. Meanwhile, the microscopic length scale is often much smaller than the characteristic length over which the macroscopic excitation varies in space. The distinct hierarchy of scales is known as the principle of scale separation. This principle states that the characteristic length scale over which the macroscopic field variables vary, should be much larger than the size of the microscopic volume considered. In other words, macroscopic quantities are nearly constant at the level of a RVE. Consequently, the presented framework looses its reliability and validity as the spatial profile of the macroscopic temperature gradient gets steeper within typical RVE sizes used in the model.

In a conventional heat conduction analysis, the conductivity tensor determining the heat flux vector is expressed in closed form in terms of material parameters and state variables which requires dedicated experimental investigations especially for heterogeneous materials. However, in computational homogenization, the heat flux vector and conductivity tensor are extracted from the solution of a micro heat flow analysis carried out at the RVE level. To elaborate the principles further, a rectangular two-dimensional RVE will be considered in the sequel, without loss of generalization to three-dimensional cases. In a computational finite element setting, at each macroscopic integration point, temperature and temperature gradient will be calculated through interpolation of the (iteratively corrected) nodal temperature data. This set of macroscopic data is used to define the boundary conditions to be imposed on the microscopic problem associated with this particular integration point. After solving the microscopic RVE BVP, the macroscopic heat flux

DOI: 10.1002/nme

is obtained by volume averaging the resulting heat flux field over the RVE and the macroscopic (tangent) conductivity is extracted from the microstructural conductivity. Due to the negligibly small size of the microstructural domain, the heat conduction at the micro level will be assumed to be insensitive to the time variations of the heat storage at this level. In other words, it may be assumed that a steady-state micro temperature profile is reached instantaneously. Additionally, the thermal constitutive behavior of each phase at the micro level is assumed to be known, which in general is governed by Fourier's law of heat conduction. On the other hand, the macroscopic heat flow problem remains completely general, i.e. transient with any kind of boundary conditions and does not require an explicitly formulated thermal constitutive behavior.

Following the proper definitions of the problem at both scales in Sections 3.1 and 3.2, the micro to macro scale transition (step I) will be elaborated in Section 4.1. Next, a consistent scheme for the micro to macro transition will be introduced in Section 4.3. The solution of the BVP at the micro level (step II) and the extraction of the macroscopic quantities (step III) will be treated in Section 5 in detail.

In what follows, the superscript or subscript 'M' denotes macroscopic quantities whereas a lower case 'm' will be the indicator for microscopic quantities, including some differential operators, e.g. the gradient operator ∇_{M} or ∇_{m}. Following conventions are used in the notations of vectors, tensors and related products:

- scalars a;
- vectors $\mathbf{a}$;
- second-order tensors $\mathbf{A}$;
- matrices and rows/columns $\underline{A}$ or $\underline{a}$;
- $\mathbf{a} \cdot \mathbf{b} = a_i b_i$; and
- $\mathbf{A} \cdot \mathbf{a} = A_{ij} a_j \mathbf{e}_{\mathrm{i}}$.

At both scales, the componentwise representation of the vectors, tensors and gradient operators are based on a common Cartesian basis with the triad, $\mathbf{e}_1, \mathbf{e}_2, \mathbf{e}_3$.

3. FORMULATION OF THE THERMAL PROBLEM AT BOTH SCALES

3.1. The micro scale problem

The micro scale problem is defined on a RVE, where physical and geometrical properties of the material microstructure components are embedded. The choice of the RVE is a delicate task, particularly for materials with random microstructures, see e.g. [25]. In this paper, it is assumed that the appropriate RVE has already been selected.

Due to negligibly small RVE size, the time variation of the heat storage may be neglected within the microstructural domain (see Section 2). This assumption leads to the steady-state micro thermal equilibrium which is expressed as

$$\nabla_{\mathrm{m}} \cdot \mathbf{q}_{\mathrm{m}}(\mathbf{x}) = 0 \tag{1}$$

where $\mathbf{q}_{\mathrm{m}}$ is the microscopic heat flux vector. In a two-dimensional context, a rectangular micro domain is shown in Figure 2. The volume of the RVE is designated by V and the boundaries, Γ, are labeled with L (left), R (right), T (top) and B (bottom). The same convention is also used for

DOI: 10.1002/nme

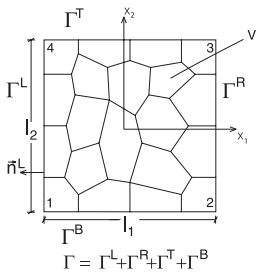

Figure 2. Micro-domain.

the unit outward normal vectors along the boundaries, e.g. $\mathbf{n}^{\mathrm{L}}$. Four corner points are numbered in counter-clockwise direction starting from the lower left corner as shown in Figure 2. For the solution of Equation (1) in V, the BVP needs to be complemented with proper boundary conditions which can be formulated in terms of a prescribed temperature or a prescribed normal heat flux on the boundary Γ. As mentioned in Section 2, the thermal characterization of the microstructural components is described by Fourier's law of heat conduction, through which the microscopic heat flux $\mathbf{q}_{\mathrm{m}}$ can be determined. It is important to note that there are no *a priori* restrictions on the specification of the constitutive laws and material parameters (e.g. constant, temperature-dependent and/or anisotropic) other than the basic thermodynamical limitations.

3.2. The macro scale problem

At the macro level, the heat balance equation takes the general time-dependent form according to

$$(\rho c_v)_{\mathrm{M}}\dot{\theta}_{\mathrm{M}} + \nabla_{\mathrm{M}} \cdot \mathbf{q}_{\mathrm{M}} = 0 \tag{2}$$

where θ_{M}, $\mathbf{q}_{\mathrm{M}}$ and $(\rho c_v)_{\mathrm{M}}$ represent the temperature, the heat flux and the heat capacity, respectively. This balance equation is to be complemented by macroscopic boundary conditions and additionally by initial conditions. Within a general setting, numerical approximation techniques (i.e. the finite element method) have to be used to solve the macroscopic heat flow problem.

Within the proposed computational homogenization procedure the heat flux is obtained from the solution of the micro-scale thermal problem, which is defined on the underlying microstructure. In addition to the macroscopic heat flux, the discretized weak form of the macroscopic governing equation requires the homogenized conductivity for the solution of the resulting system of equations. The evaluation of the macroscopic heat flux and the extraction of the macroscopic conductivity are elaborated in the following sections.

For the determination of the macroscopic heat storage to be substituted in Equation (2), the following volume averaging is proposed:

$$(\rho c_v)_{\mathrm{M}} = \frac{1}{V}\int_V (\rho c_v)_{\mathrm{m}}\,\mathrm{d}V \tag{3}$$

which can be also obtained by the asymptotic homogenization method as done in [6]. This equation reflects that the heat capacity is consistently preserved upon scale bridging. In a computational context, in addition to the macroscopic heat flux and the conductivity, also the macroscopic

DOI: 10.1002/nme

volumetric heat capacity parameter, i.e. $(\rho c_v)_{\mathrm{M}}$ in Equation (3) should be extracted from the micro level in case of a macroscopically transient problem.

4. SCALE TRANSITIONS

4.1. The macro–micro scale transition

Within the framework of a multi-scale analysis, the actual microscopic temperature profile, $\theta_{\mathrm{m}}(\mathbf{x})$ with $\mathbf{x}$ the position vector, can be decomposed without loss of generality in a spatially linear mean (macroscopic) field and a fluctuation field $\theta_{\mathrm{f}}(\mathbf{x})$ as

$$\theta_{\mathrm{m}}(\mathbf{x}) = \theta_{\mathrm{m}}^{k} + \nabla_{\mathrm{M}}\theta_{\mathrm{M}} \cdot (\mathbf{x} - \mathbf{x}^{k}) + \theta_{\mathrm{f}}(\mathbf{x}) \tag{4}$$

which can be interpreted as a perturbation of a mean (macroscopic) field with a fluctuation at the micro scale due to variations in material properties (e.g. conductivity) within the RVE. In Equation (4), θ_{m}^{k} is the temperature at an arbitrary point, $\mathbf{x}^{k}$, within the RVE and yet undetermined.

More conveniently, the microscopic temperature profile can be expressed with respect to the temperature value of corner 1 according to

$$\theta_{\mathrm{m}}(\mathbf{x}) = \theta_{\mathrm{m}}^{1} + \nabla_{\mathrm{M}}\theta_{\mathrm{M}} \cdot (\mathbf{x} - \mathbf{x}^{1}) + \theta_{\mathrm{f}}(\mathbf{x}) \tag{5}$$

which can simply be accomplished using the difference of the temperature value of corner 1 and the temperature value of any other arbitrary point according to Equation (4). In Equation (5), θ_{m}^{1} is the microscopic temperature value at corner 1 with position vector $\mathbf{x}^{1}$.

The temperature profile at the micro level results from the imposed boundary conditions and the distinct conductivities of the microstructural phases, which may be temperature-dependent. Therefore, the determination of the reference temperature in the micro domain, which has been indicated by θ_{m}^{1}, is important for an adequate and unique solution. To this end, an additional constraint, which enforces the consistency of the stored heat at the macro and the micro level is proposed

$$(\rho c_v)_{\mathrm{M}}\theta_{\mathrm{M}} = \frac{1}{V}\int_{V} (\rho c_v)_{\mathrm{m}}\theta_{\mathrm{m}}\,\mathrm{d}V \tag{6}$$

in addition to the macroscopic heat capacity already introduced in Equation (3). This condition is sufficient to obtain a unique temperature profile and enforces a temperature distribution that respects the consistency of the stored heat at micro and macro level. It will be referred to as the thermal energy consistency condition in the following sections.

The driving mechanism for heat conduction is the temperature gradient developing in the volume as a result of the boundary conditions. Therefore, an important characteristic of the scale transition between the micro and the macro level is the transfer of temperature gradients. Recalling that the temperature field is additively split in its macro and micro contributions (see Equation (4)) the volume averaged micro temperature gradient can be written as

$$\frac{1}{V}\int_{V} \nabla_{\mathrm{m}}\theta_{\mathrm{m}}\,\mathrm{d}V = \nabla_{\mathrm{M}}\theta_{\mathrm{M}} + \frac{1}{V}\int_{\Gamma} \theta_{\mathrm{f}}\mathbf{n}\,\mathrm{d}\Gamma \tag{7}$$

where the volume integral involving the fluctuation field is converted into a boundary (Γ) integral with the aid of the Gauss divergence theorem.

DOI: 10.1002/nme

The gradient $\nabla_{\mathrm{M}}\theta_{\mathrm{M}}$ reflects the thermal effect of the macroscopic heat flow which has to be transferred through the boundary conditions to the RVE. A scale transition relation that enforces the macroscopic temperature gradient to equal the volume average of its microscopic counterpart is therefore introduced. This condition leads to the constraint

$$\int_{\Gamma} \theta_{\mathrm{f}}\mathbf{n}\,\mathrm{d}\Gamma = \mathbf{0} \tag{8}$$

which can be satisfied by different sets of RVE boundary conditions.

4.2. Micro-scale RVE boundary conditions

If the scale transition constraint (8) is written explicitly as

$$\int_{\Gamma^{\mathrm{L}}} \{\theta_{\mathrm{f}}^{\mathrm{L}} - \theta_{\mathrm{f}}^{\mathrm{R}}\}\mathbf{n}^{\mathrm{L}}\,\mathrm{d}\Gamma + \int_{\Gamma^{\mathrm{B}}} \{\theta_{\mathrm{f}}^{\mathrm{B}} - \theta_{\mathrm{f}}^{\mathrm{T}}\}\mathbf{n}^{\mathrm{B}}\,\mathrm{d}\Gamma = \mathbf{0} \tag{9}$$

it is immediately clear that the sufficient conditions, in terms of macroscopic and microscopic quantities, can be formulated as

$$\theta_{\mathrm{m}}^{\mathrm{R}} - \theta_{\mathrm{m}}^{\mathrm{L}} = \nabla_{\mathrm{M}}\theta_{\mathrm{M}} \cdot (\mathbf{x}^{\mathrm{R}} - \mathbf{x}^{\mathrm{L}}) \tag{10a}$$

$$\theta_{\mathrm{m}}^{\mathrm{T}} - \theta_{\mathrm{m}}^{\mathrm{B}} = \nabla_{\mathrm{M}}\theta_{\mathrm{M}} \cdot (\mathbf{x}^{\mathrm{T}} - \mathbf{x}^{\mathrm{B}}) \tag{10b}$$

These are the so-called periodic boundary conditions which naturally result in anti-periodic normal flux boundary conditions

$$q_{\mathrm{m}_n}^{\mathrm{L}} = -q_{\mathrm{m}_n}^{\mathrm{R}} \tag{11a}$$

$$q_{\mathrm{m}_n}^{\mathrm{T}} = -q_{\mathrm{m}_n}^{\mathrm{B}} \tag{11b}$$

according to the heat flux balance. In Equation (11) the normal heat flux components over the boundaries, $q_{\mathrm{m}_n}^{(\mathrm{L,R,T,B})}$, are defined as

$$q_{\mathrm{m}_n}^{(\mathrm{L,R,T,B})} = \mathbf{q}_{\mathrm{m}}^{(\mathrm{L,R,T,B})} \cdot \mathbf{n}^{(\mathrm{L,R,T,B})} \tag{12}$$

It is trivial that under steady-state conditions the inflowing heat flux should be equal to the outgoing flux.

Based on the macro to micro transition structure, different boundary conditions satisfying Equation (8) can be constructed, e.g. $\theta_{\mathrm{f}} = 0$ on Γ for prescribed temperature boundary conditions. Alternatively, it is possible to prescribe flux boundary conditions in terms of the macroscopic heat flux. However, in the sequel of this paper, periodic boundary conditions will be used, since it is known that they provide the best approximation for a fixed RVE size in a purely mechanical analysis, see e.g. [26]. Note that the periodic boundary conditions have a purely mathematical motivation and therefore do not imply any kind of geometric restrictions on the micro-domain, e.g. geometrically periodic RVE.

DOI: 10.1002/nme

4.3. The micro–macro scale transition

The second law of thermodynamics leads to Fourier's inequality, in its standard form given by

$$-\frac{1}{\theta}\nabla\theta\cdot\mathbf{q}\geqslant 0 \tag{13}$$

which is essentially the entropy change due to heat conduction. Eliminating the temperature appearing in the denominator (as proposed in [27]) and enforcing the consistency of the entropy change at the macro and the micro level, one can write

$$\frac{1}{V}\int_V \nabla_{\mathrm{m}}\theta_{\mathrm{m}}\cdot\mathbf{q}_{\mathrm{m}}\,\mathrm{d}V=\nabla_{\mathrm{M}}\theta_{\mathrm{M}}\cdot\mathbf{q}_{\mathrm{M}} \tag{14}$$

stating that the entropy change due to heat conduction at the macroscopic point level should be consistent with that of the underlying microstructure. Since the scale bridging relation for the temperature gradient is already introduced, according to Equations (7) and (8), the entropy consistency condition constitutes the basis for linking micro and macro heat flux fields. For the following considerations, it is more appropriate to transform the left-hand side of Equation (14) according to

$$\frac{1}{V}\int_V \nabla_{\mathrm{m}}\theta_{\mathrm{m}}\cdot\mathbf{q}_{\mathrm{m}}\,\mathrm{d}V=\frac{1}{V}\int_\Gamma \theta_{\mathrm{m}}q_{\mathrm{m}_n}\,\mathrm{d}\Gamma \tag{15}$$

for which the identity $\nabla_{\mathrm{m}}\cdot(\theta_{\mathrm{m}}\mathbf{q}_{\mathrm{m}})=\nabla_{\mathrm{m}}\theta_{\mathrm{m}}\cdot\mathbf{q}_{\mathrm{m}}$ due to the balance of heat, has been used.

Additionally, to be exploited in the following, the volume averaged microscopic heat flux field can be written as

$$\frac{1}{V}\int_V \mathbf{q}_{\mathrm{m}}\,\mathrm{d}V=\frac{1}{V}\int_\Gamma \mathbf{x}q_{\mathrm{m}_n}\,\mathrm{d}\Gamma \tag{16}$$

with the aid of the identity

$$\nabla_{\mathrm{m}}\cdot(\mathbf{x}_{\mathrm{m}}\mathbf{q}_{\mathrm{m}})=\nabla_{\mathrm{m}}\mathbf{x}_{\mathrm{m}}\cdot\mathbf{q}_{\mathrm{m}}+\mathbf{x}_{\mathrm{m}}(\nabla_{\mathrm{m}}\cdot\mathbf{q}_{\mathrm{m}})=\mathbf{q}_{\mathrm{m}} \tag{17}$$

which holds in view of the heat balance and the identity $\nabla_{\mathrm{m}}\mathbf{x}_{\mathrm{m}}=\mathbf{I}$. In the case of periodic temperature and the associated anti-periodic normal heat flux boundary conditions, the volume averaged micro entropy change (the right-hand side of Equation (15)) can be expressed as

$$\begin{aligned}\frac{1}{V}\int_\Gamma \theta_{\mathrm{m}}q_{\mathrm{m}_n}\,\mathrm{d}\Gamma&=\frac{1}{V}\nabla_{\mathrm{M}}\theta_{\mathrm{M}}\cdot\int_{\Gamma^{\mathrm{L}}}(\mathbf{x}_{\mathrm{L}}-\mathbf{x}_{\mathrm{R}})\mathbf{q}_{\mathrm{m}}\cdot\mathbf{n}^{\mathrm{L}}\,\mathrm{d}\Gamma+\frac{1}{V}\nabla_{\mathrm{M}}\theta_{\mathrm{M}}\cdot\int_{\Gamma^{\mathrm{B}}}(\mathbf{x}_{\mathrm{B}}-\mathbf{x}_{\mathrm{T}})\mathbf{q}_{\mathrm{m}}\cdot\mathbf{n}^{\mathrm{B}}\,\mathrm{d}\Gamma\\&=\nabla_{\mathrm{M}}\theta_{\mathrm{M}}\cdot\frac{1}{V}\int_\Gamma \mathbf{x}q_{\mathrm{m}_n}\,\mathrm{d}\Gamma=\nabla_{\mathrm{M}}\theta_{\mathrm{M}}\cdot\frac{1}{V}\int_V \mathbf{q}_{\mathrm{m}}\,\mathrm{d}V\end{aligned} \tag{18}$$

Comparing Equation (18) with Equations (14) and (15) leads to the identification

$$\frac{1}{V}\int_V \mathbf{q}_{\mathrm{m}}\,\mathrm{d}V=\mathbf{q}_{\mathrm{M}} \tag{19}$$

showing the equivalence of the volume averaged micro heat flux field and the macroscopic heat flux. If investigated for other boundary conditions, the scale bridging strategy leads to the same consistent result that the macroscopic heat flux is equal to the volume averaged microscopic heat flux field over the RVE domain.

DOI: 10.1002/nme

5. TWO-SCALE NUMERICAL SOLUTION STRATEGY

Once the boundary conditions for the RVE and the constitutive laws for each constituent of the microstructure are defined, the BVP at the micro level can be solved by the finite element method numerically. The two-dimensional RVE problem will be elaborated, where its extension to three-dimension is relatively straightforward.

5.1. RVE boundary value problem

The discretization of the weak form of the microscopic heat balance equation leads to a system of (non-)linear algebraic equations in the unknown nodal temperatures stored in the column $\underline{\theta}$, which can be written as

$$\underline{q}_{\text{int}}(\underline{\theta}) = \underline{q}_{\text{ext}} \tag{20}$$

Equation (20) states that the externally applied nodal heat fluxes are equilibrated by the nodal internal fluxes. The system is excited by the macroscopic loading term $\underline{\Upsilon}_{\text{M}}$, a column consisting of the macroscopic temperature and the components of the macroscopic temperature gradient with respect to the base vectors $\{\mathbf{e}_1, \mathbf{e}_2\}$

$$\underline{\Upsilon}_{\text{M}} = \begin{bmatrix} \theta_{\text{M}} \\ (\nabla_{\text{M}}\theta_{\text{M}})_1 \\ (\nabla_{\text{M}}\theta_{\text{M}})_2 \end{bmatrix} \tag{21}$$

According to the scale separation adopted, these quantities remain constant at the level of the microscopic problem for a single macroscopic incremental iteration. The temperature column is next decomposed in, $\underline{\theta}_{\text{e}}$, the nodal temperatures at the edge nodes (excluding nodes located at the four corners of the RVE), $\underline{\theta}_{\text{i}}$, internal nodal temperatures (excluding nodes located at the RVE boundaries) and $\underline{\theta}_{\text{c}}$, the nodal temperatures of the corner nodes. The columns $\underline{q}_{\text{int}}$ and $\underline{q}_{\text{ext}}$ are split up likewise. In case of temperature-dependent conductivities at the micro level, the equilibrium solution satisfying Equation (20) can be obtained iteratively using a classical Newton–Raphson scheme. To this purpose, the system of equations (20) is linearized with respect to the incremental estimates $\underline{\theta}^k$, which yields the following system for the iterative corrections $\delta\underline{\theta}$:

$$\underline{K}\,\delta\underline{\theta} = \underline{q}_{\text{ext}} - \underline{q}_{\text{int}}(\underline{\theta}^k) \tag{22}$$

where the matrix $\underline{K}$ is defined by

$$\underline{K} = \left.\frac{\partial \underline{q}_{\text{int}}}{\partial \underline{\theta}}\right|_{\underline{\theta}^k} \tag{23}$$

The resulting system of equations takes the following decomposed format:

$$\begin{bmatrix} \underline{K}_{\text{ee}} & \underline{K}_{\text{ei}} & \underline{K}_{\text{ec}} \\ \underline{K}_{\text{ie}} & \underline{K}_{\text{ii}} & \underline{K}_{\text{ic}} \\ \underline{K}_{\text{ce}} & \underline{K}_{\text{ci}} & \underline{K}_{\text{cc}} \end{bmatrix} \begin{bmatrix} \delta\underline{\theta}_{\text{e}} \\ \delta\underline{\theta}_{\text{i}} \\ \delta\underline{\theta}_{\text{c}} \end{bmatrix} = \begin{bmatrix} \underline{q}_{\text{e}}^{\text{ext}} \\ \underline{0} \\ \underline{q}_{\text{c}}^{\text{ext}} \end{bmatrix} - \begin{bmatrix} \underline{q}_{\text{e}}^{\text{int}}(\underline{\theta}^k) \\ \underline{q}_{\text{i}}^{\text{int}}(\underline{\theta}^k) \\ \underline{q}_{\text{c}}^{\text{int}}(\underline{\theta}^k) \end{bmatrix} \tag{24}$$

DOI: 10.1002/nme

To proceed further, the column $\underline{\theta}_e$ is subdivided in a first subcolumn with the independent values $\underline{\theta}_n$ containing the nodal temperature unknowns of the left and bottom edges and a second subcolumn with the dependent degrees of freedom $\underline{\theta}_d$ (i.e. the nodal temperature unknowns of the right and top edges which will be eliminated by a master–slave approach *via* tying relations). To ease the implementation, the RVE domain is discretized in such a way that the nodes on opposite sides match geometrically. The periodic boundary conditions applied to the edge nodes lead to a set of constraints of a non-homogeneous type which can be expressed as

$$\underline{\theta}_r = \underline{\theta}_l + \underline{C}_{rl}\,\underline{\Upsilon}_M \tag{25a}$$

$$\underline{\theta}_t = \underline{\theta}_b + \underline{C}_{tb}\,\underline{\Upsilon}_M \tag{25b}$$

where $\underline{C}_{rl}$ and $\underline{C}_{tb}$ are the coefficient matrices of the tying relations, resulting from Equation (10). Consequently, the edge degrees of freedom $\underline{\theta}_e$ can be expressed as

$$\underline{\theta}_e = \underline{T}\,\underline{\theta}_n + \underline{G}\,\underline{\Upsilon}_M \tag{26}$$

where the matrices $\underline{T}$ and $\underline{G}$ are implicitly defined through the above relations. Note that periodicity assumption induces that the external nodal heat flux column $\underline{q}_e^{ext}$ on the right-hand side of Equation (24) reflects anti-periodicity (see Equation (11)). Using this information and the introduced transformation (Equation (26)), equation system (24) can be condensed to the following form:

$$\begin{bmatrix} \underline{T}^T\underline{K}_{ee}\underline{T} & \underline{T}^T\underline{K}_{ei} & \underline{T}^T\underline{K}_{ec} \\ \underline{K}_{ie}\underline{T} & \underline{K}_{ii} & \underline{K}_{ic} \\ \underline{K}_{ce}\underline{T} & \underline{K}_{ci} & \underline{K}_{cc} \end{bmatrix} \begin{bmatrix} \delta\underline{\theta}_n \\ \delta\underline{\theta}_i \\ \delta\underline{\theta}_c \end{bmatrix} = \begin{bmatrix} -\underline{q}_n^{int} - \underline{q}_d^{int} \\ -\underline{q}_i^{int} \\ \underline{q}_c^{ext} - \underline{q}_c^{int} \end{bmatrix} \tag{27}$$

$\underline{q}_n^{int}$ and $\underline{q}_d^{int}$ appearing on the right-hand side are the corresponding subcolumns of the internal nodal heat flux column of edge nodes introduced as $\underline{q}_e^{int}$ in Equation (24). Due to the structure of the transformation matrix $\underline{T}^T$ and the anti-periodicity condition, the non-zero entries of the column $\underline{q}_e^{ext}$ cancel out and therefore do not appear in equation system (27). Note that, variations, $\delta\underline{\theta}_e$, are purely expressed in $\delta\underline{\theta}_n$ since the variations of the macroscopic quantities, $\delta\,\underline{\Upsilon}_M$, are zero upon solving the micro problem. Further on, the periodic temperature boundary conditions for the corner nodes lead to three independent equations according to

$$\theta^2 = \theta^1 + (\underline{\Upsilon}_M)_2 l_1 \tag{28a}$$

$$\theta^3 = \theta^1 + (\underline{\Upsilon}_M)_2 l_1 + (\underline{\Upsilon}_M)_3 l_2 \tag{28b}$$

$$\theta^4 = \theta^1 + (\underline{\Upsilon}_M)_3 l_2 \tag{28c}$$

Finally, the equation system is completed by the stored heat consistency condition (Equation (6)), which, upon discretization, can be written as

$$\underline{C}\,\underline{\theta} = (\underline{\Upsilon}_M)_1 \tag{29}$$

DOI: 10.1002/nme

where $\underline{C}$ is the coefficient row corresponding to this constraint. In a variational form, the four equations (Equations (28) and (29)) can be compactly expressed as

$$[\underline{M}_{\mathrm{ce}} \;\; \underline{M}_{\mathrm{ci}} \;\; \underline{M}_{\mathrm{cc}}] \begin{bmatrix} \delta\underline{\theta}_{\mathrm{e}} \\ \delta\underline{\theta}_{\mathrm{i}} \\ \delta\underline{\theta}_{\mathrm{c}} \end{bmatrix} = [\underline{M}_{\mathrm{ce}}\underline{T} \quad \underline{M}_{\mathrm{ci}} \quad \underline{M}_{\mathrm{cc}}] \begin{bmatrix} \delta\underline{\theta}_{\mathrm{n}} \\ \delta\underline{\theta}_{\mathrm{i}} \\ \delta\underline{\theta}_{\mathrm{c}} \end{bmatrix} = \underline{0} \tag{30}$$

where the matrices $\underline{M}_{(\mathrm{ce,ci,cc})}$ contain the coefficients corresponding to this set of constraints. By replacing the last four (corner node) equations in (27) by the set of four equations (30), the resulting system can be solved in a straightforward manner since the right-hand side is known. Using this solution, the column $\underline{\theta}$ is updated followed by a re-evaluation of the internal nodal fluxes. The iterative process is repeated until the right-hand side gets sufficiently small.

5.2. *Extraction of the macroscopic heat flux*

After a microstructural heat conduction analysis has been performed, the macroscopic heat flux vector is extracted through volume averaging. This is done by numerically evaluating the boundary integral in the right-hand side of Equation (16) which will be further simplified in the following.

With the aid of the anti-periodic heat flux boundary conditions (see Equation (11)), Equation (16) can be formulated as

$$\mathbf{q}_{\mathrm{M}} = (\mathbf{x}_{\mathrm{L}} - \mathbf{x}_{\mathrm{R}}) \int_{\Gamma_{\mathrm{L}}} q^{\mathrm{L}}_{\mathrm{m}_n} \, \mathrm{d}\Gamma + (\mathbf{x}_{\mathrm{B}} - \mathbf{x}_{\mathrm{T}}) \int_{\Gamma_{\mathrm{B}}} q^{\mathrm{R}}_{\mathrm{m}_n} \, \mathrm{d}\Gamma + \mathbf{x}_{\mathrm{c}} \underline{q}^{\mathrm{ext}}_{\mathrm{c}} \tag{31}$$

which, upon discretization and due to thermal equilibrium, takes the following final form:

$$\mathbf{q}_{\mathrm{M}} = \frac{1}{V}((\mathbf{x}_{\mathrm{L}} - \mathbf{x}_{\mathrm{R}}) \sum \underline{q}^{\mathrm{ext}}_{\mathrm{L}} + (\mathbf{x}_{\mathrm{B}} - \mathbf{x}_{\mathrm{T}}) \sum \underline{q}^{\mathrm{ext}}_{\mathrm{B}} + \underline{\mathbf{x}}_{\mathrm{c}} \underline{q}^{\mathrm{ext}}_{\mathrm{c}}) \tag{32}$$

In Equation (32), $\underline{q}^{\mathrm{ext}}_{\mathrm{L}}$ and $\underline{q}^{\mathrm{ext}}_{\mathrm{B}}$ are the columns of nodal heat fluxes developing at the left and bottom edges, respectively. Using the obtained complete nodal temperature column $\underline{\theta}$ at the micro level, the internal and external nodal heat flux columns can be obtained by simple substitution into Equation (20). The summations in Equation (32) are to be performed over the components of the corresponding columns. The last term $\underline{\mathbf{x}}_{\mathrm{c}} \underline{q}^{\mathrm{ext}}_{\mathrm{c}}$ (with $\underline{\mathbf{x}}_{\mathrm{c}}$, a row with corner node position vectors) represents the contribution of the heat fluxes at the corner nodes. Equation (32) can be conveniently expressed in a matrix-column format as

$$\underline{q}_{\mathrm{M}} = [\underline{L}_{\mathrm{n}} \;\; \underline{L}_{\mathrm{c}}] \begin{bmatrix} \underline{q}^{\mathrm{ext}}_{\mathrm{n}} \\ \underline{q}^{\mathrm{ext}}_{\mathrm{c}} \end{bmatrix} \tag{33}$$

where $\underline{L}_{\mathrm{n}}$ and $\underline{L}_{\mathrm{c}}$ are implicitly defined. Equation (33) is exploited for the evaluation of the macroscopic heat flux. In the next section, this expression will be used as the point of departure for the calculation of the macroscopic (tangent) conductivity.

5.3. *Extraction of the macroscopic conductivity*

To solve the macroscopic problem, a relation between the variation of the macroscopic heat flux and the variation of the macroscopic temperature gradient in the form

$$\delta \underline{q}_{\mathrm{M}} = \underline{K}_{\mathrm{M}} \delta(\underline{\nabla}_{\mathrm{M}} \theta_{\mathrm{M}}) \tag{34}$$

DOI: 10.1002/nme

should be constructed, where $\underline{K}_{\mathrm{M}}$ is the macroscopic (tangent) conductivity at integration point level of the macroscopic discretization. To this end, the variation of the macroscopic heat flux expression in its matrix-column format (Equation (33)) is taken:

$$\delta \underline{q}_{\mathrm{M}} = [\,\underline{L}_{\mathrm{n}} \;\; \underline{L}_{\mathrm{c}}\,] \begin{bmatrix} \delta \underline{q}_{\mathrm{n}}^{\mathrm{ext}} \\ \delta \underline{q}_{\mathrm{c}}^{\mathrm{ext}} \end{bmatrix} \tag{35}$$

Although $\underline{\Upsilon}_{\mathrm{M}}$ was fixed during incremental iterations at the microscopic level, the converged micro equilibrium state can be used to determine the effect of the variations in the macroscopic quantities on the resulting micro heat flux field. Obviously, this step is essential for the determination of the macroscopic conductivity. Therefore, Equation (26) is again linearized, but this time with the variation $\delta\Upsilon$ included:

$$\delta \underline{\theta}_{\mathrm{e}} = \underline{T}\, \delta \underline{\theta}_{\mathrm{n}} + \underline{G}\, \delta \underline{\Upsilon}_{\mathrm{M}} \tag{36}$$

This variation is substituted into Equation (24) where the right-hand side vanishes since the conductivity terms in (24) are taken in a converged state of the RVE problem. Condensation of the result, using the anti-periodicity conditions, (Equation (11)) reveals

$$\begin{bmatrix} \underline{T}^{\mathrm{T}} \underline{K}_{\mathrm{ee}} \underline{T} & \underline{T}^{\mathrm{T}} \underline{K}_{\mathrm{ei}} & \underline{T}^{\mathrm{T}} \underline{K}_{\mathrm{ec}} \\ \underline{K}_{\mathrm{ie}} \underline{T} & \underline{K}_{\mathrm{ii}} & \underline{K}_{\mathrm{ic}} \\ \underline{K}_{\mathrm{ce}} \underline{T} & \underline{K}_{\mathrm{ci}} & \underline{K}_{\mathrm{cc}} \end{bmatrix} \begin{bmatrix} \delta \underline{\theta}_{\mathrm{n}} \\ \delta \underline{\theta}_{\mathrm{i}} \\ \delta \underline{\theta}_{\mathrm{c}} \end{bmatrix} = - \begin{bmatrix} \underline{T}^{\mathrm{T}} \underline{K}_{\mathrm{ee}} \underline{G} \\ \underline{K}_{\mathrm{ie}} \underline{G} \\ \underline{K}_{\mathrm{ce}} \underline{G} \end{bmatrix} \delta \underline{\Upsilon}_{\mathrm{M}} \tag{37}$$

from which, the variations $\delta \underline{q}_{\mathrm{n}}^{\mathrm{ext}}$ and $\delta \underline{q}_{\mathrm{c}}^{\mathrm{ext}}$ can be extracted as

$$\begin{bmatrix} \delta \underline{q}_{\mathrm{n}}^{\mathrm{ext}} \\ \delta \underline{q}_{\mathrm{c}}^{\mathrm{ext}} \end{bmatrix} = \begin{bmatrix} -\underline{T}^{\mathrm{T}} \underline{K}_{\mathrm{ee}} \underline{G} \\ -\underline{K}_{\mathrm{ce}} \underline{G} \end{bmatrix} \delta \underline{\Upsilon}_{\mathrm{M}} \tag{38}$$

Using this information in Equation (35) finally yields the macroscopic tangent conductivity as

$$\underline{K}_{\mathrm{M}} = (-\underline{L}_{\mathrm{n}}\, \underline{T}^{\mathrm{T}}\, \underline{K}_{\mathrm{ee}}\, \underline{G} - \underline{L}_{\mathrm{c}}\, \underline{K}_{\mathrm{ce}}\, \underline{G}) \tag{39}$$

5.4. Nested solution strategy

After having examined each of the ingredients of the homogenization scheme separately, the global algorithmic framework is outlined in the following.

The temperature field on the macroscopic domain is spatially discretized by finite elements and in case of transient problems, a proper numerical time integration scheme is introduced to convert the governing differential equations into a fully discrete form. Thermal boundary conditions are parameterized in a (pseudo-)time setting and applied incrementally. For transient cases, the macroscopic problem should be complemented by initial conditions. Assuming that the time discretization is done in a convenient way, the (non-)linear equations resulting from the heat balance have to be solved with an incremental-iterative (if necessary) solution procedure. To incorporate the constitutive behavior (relating the macroscopic temperature gradient and the macroscopic heat flux), a RVE is attributed to each macroscopic integration point which is subdivided in finite elements.

DOI: 10.1002/nme

At the micro level, the macroscopic temperature gradient is used to formulate the boundary conditions to be imposed on the RVE and the macroscopic temperature is supplied to the thermal energy consistency condition rendering the microscopic temperature profile unique. Upon the solution, the macroscopic heat flux vector and the macroscopic conductivity are extracted as outlined in Section 5 and transferred to the macroscopic level (integration point). In case of transient problems, the macroscopic heat capacity is calculated through volume averaging (Equation (3)) and also passed to the macro level.

Upon completing the RVE computations, the macroscopic heat flux vector and the macroscopic heat capacity are available at each integration point and the macroscopic nodal heat balance can be evaluated. If the heat balance is satisfied (within the limits set by a predefined convergence criterion), the next time increment can be computed. Otherwise, the iterative macroscopic temperature field has to be updated using the macroscopic (tangent) conductivities which are already available in each integration point from the micro level analysis.

The high computational effort can be reduced by parallel computing which has a simple algorithmic structure due to the proposed solution procedure. In a parallel computing framework, the macroscopic mesh (data) is handled by a single master processor and the micro level problems are distributed to the slave processors which receive (RVE input) and send data (RVE output) to the master processor. The slave processors do not need to communicate with each other and therefore the parallel algorithm turns out to be very effective and simple, see [20, 21] for equivalent mechanical problems.

6. TWO-SCALE HOMOGENIZATION EXAMPLES

The proposed algorithm is implemented in a commercial finite element software framework (MSC Marc) through user-defined material routines. To illustrate the applicability of the proposed method and to emphasize its added value, two examples are worked out in this section.

For both examples the time integration is achieved by the backward-Euler integration scheme.

6.1. Thermal homogenization in a cellular foam-like structure

The first problem analyses the temperature evolution through the thickness of a wall, which serves as a separation and fire retardance unit and which is made of a closed-cell aluminum foam. The structural details and boundary conditions are depicted in Figure 3. Due to the assumed boundary conditions, the macroscopic system can be modeled as a one-dimensional heat conduction problem over the wall thickness of 150 mm. On the outer side of the wall, a convection boundary condition with a film coefficient of 50 $\mathrm{W/m^2\,K}$ is used, combined with an ambient temperature $T_0 = 20°\mathrm{C}$. The inner face of the wall is exposed to a final temperature T_f equal to 400°C starting from an initial temperature of 20°C. The final temperature level is reached in 1 s and it is kept constant thereafter, see the left-hand side of Figure 3. A typical strip of the macroscopic domain is discretized by 32 four-noded quadrilateral elements with four integration points (total dofs = 66) and a constant time step size of 0.5 is used. The microscopic mesh consists of 652 elements (total dofs = 702).

Aluminum foams have favorable heat isolating and fire retardance properties and are classified by their basic cell geometry. Here, a perfect hexagonal geometry ($h = l$) is considered, see Figure 3, with a relative density equal to 0.05, which is essentially the ratio of solid volume with respect

DOI: 10.1002/nme

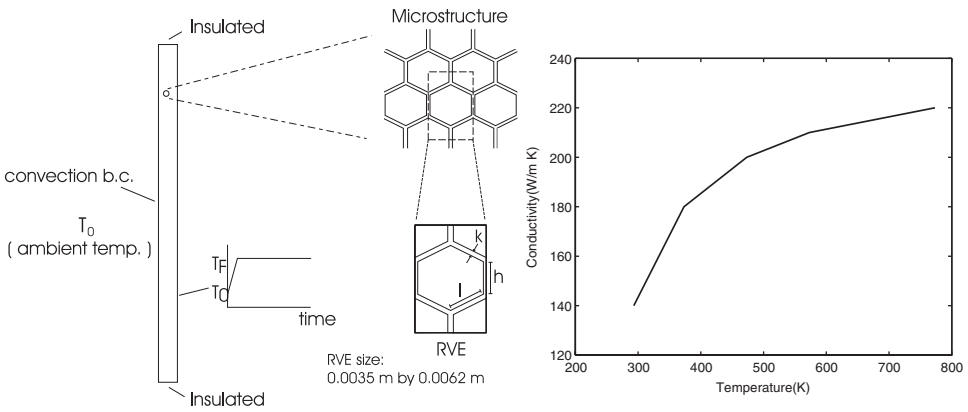

Figure 3. Typical hexagonal structure and the representative volume element (i.e. a unit cell) selected.

to the total cell volume. In reality, three mechanisms of heat transfer (conduction, convection and radiation) take place at the micro level. For the geometry and the cell type as selected here, the contribution of convection and radiation can be neglected (see [28] for details). Therefore, a hexagonal RVE composed of a solid skeleton and air through which heat can be transferred by conduction only is considered. Both constant- and temperature-dependent conductivities are considered. For the temperature-dependent case, a temperature *vs* conductivity relation is given in the right-hand side of Figure 3, showing an improved conductivity at increasing temperature. In the constant conductivity case, a conductivity of 200 W/mK is taken for the solid skeleton, which is the value corresponding to approximately 200°C in Figure 3. For air, the conductivity value is taken as 0.025 W/mK. For the solid skeleton, the density and heat capacity values are taken to be 2700 kg/m^3 and 940 J/kg K respectively. For air, the values used are 1.25 kg/m^3 and 1005 J/kg K, respectively. Therefore memory effects mentioned in [6] do not appear since the ratio $(c_v)_{\text{air}}/(c_v)_{\text{alum}}$ is also low, see [6] for the details. For constant conductivity case, the computation time can be reduced extensively since it is sufficient to obtain the homogenized conductivity just once from the analysis of the microstructure under arbitrary loading conditions. Therefore, the computational cost for constant conductivity case is comparable with that of a conventional finite element analysis. However, in case of temperature-dependent conductivities at the micro level, the computational cost increases considerably, for this particular case approximately 40 h on a single processor machine for 150 time steps. In Figure 4, a comparison of temperature profiles at different times, for a constant and for a temperature-dependent conductivity is presented. For comparison purposes, the result based on the conductivity obtained from the rule of mixtures (using the constant average conductivity) is also presented. It is clear from Figure 4 that the comparison of constant conductivity case and the rule of mixtures results reveals that the rule of mixture solution overestimates the temperature values considerably.

For the constant conductivity case, a good agreement between the macroscopic conductivity obtained here and the one given in Reference [29] is obtained. The latter results are based on an analytical approach mainly valid for small k/l (k: thickness of the solid skeleton, see Figure 3) ratios. However, for larger k/l ratios, the analytical model [29] and our findings deviate since the analytical model is based on a one-dimensional heat conduction along the solid skeleton parts.

DOI: 10.1002/nme

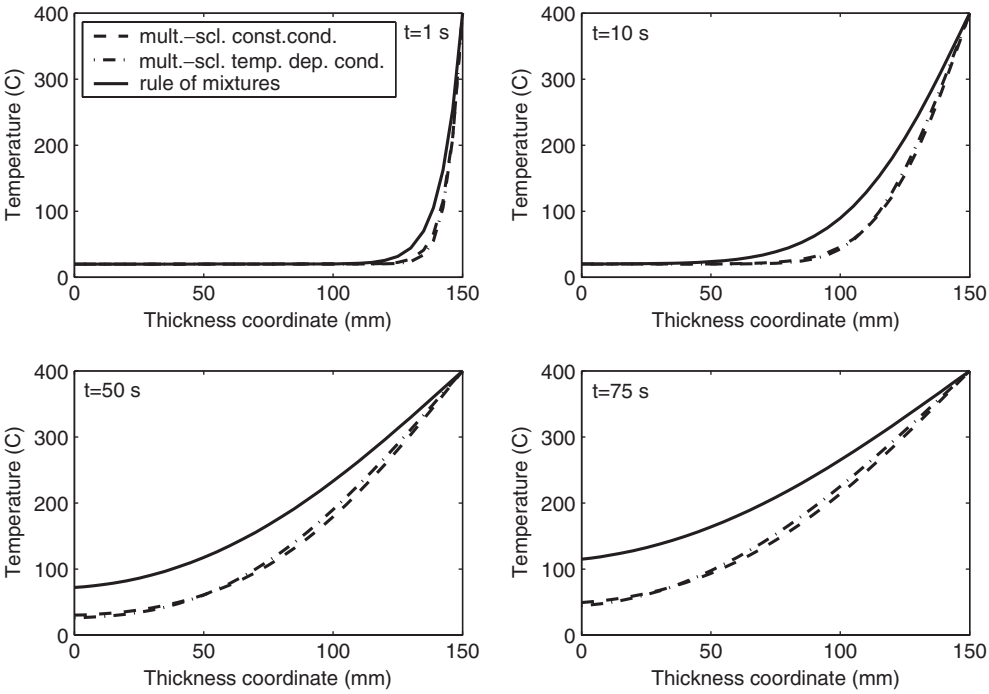

Figure 4. Comparison of temperature profiles over the thickness at different times.

6.2. Thermal homogenization in refractory-like materials

The second problem specification is inspired by the furnace linings used in steel production plants. Typically, refractory bricks with a granular microstructure are used for the linings. Due to the production stages and an inherent anisotropic (mechanically and thermally) granular structure, a material microstructure composed of discretely connected (or disconnected) grains with different principal heat conduction directions should be dealt with. Schematically, the rotated coordinate systems, see Figure 5, represent the anisotropy of each grain of the microstructure. To obtain a better understanding of the effect of the anisotropy, two different cases are considered. In the first case, the scatter of the principal directions between the grains is taken to be small. This reflects a strong texture, where the principal directions of any grain are close to those of the neighboring grains, the difference lying within a range of 10°. In the second case, the principal directions of the grains are taken randomly. Additionally, to make a comparison, the temperature profile is also computed using the conductivities obtained by the rule of mixtures. Further on, to investigate qualitatively the effect of thermomechanical damage (i.e. disconnected grains) due to abrupt temperature changes and cycles, a pre-damaged RVE with a diagonal crack (see Figure 5) is introduced. The domain within the crack is assumed to have the properties of air which are already given in the previous example. The structure is modeled as a two-dimensional problem with boundary conditions as indicated in Figure 5. Starting from an initial temperature of 20°C, the inner faces of the structure are exposed to a final temperature of 800°C, reached in 2 s and kept constant thereafter. The reference conductivity tensor is taken to be orthotropic with principal

DOI: 10.1002/nme

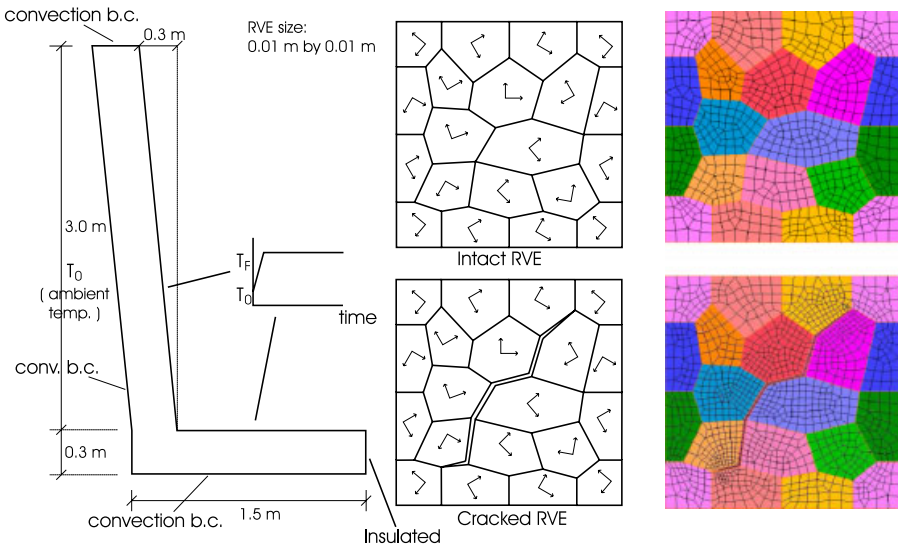

Figure 5. The Ladle structure and RVE composed of grains with an anisotropic heat conductivity.

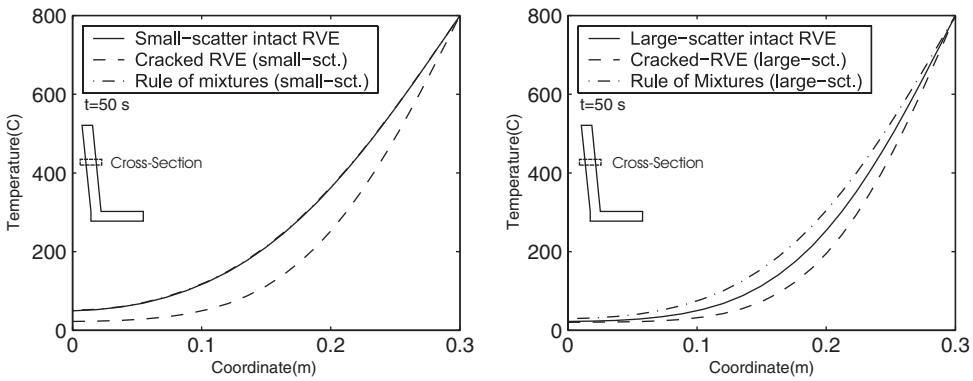

Figure 6. Comparison of the temperature distribution for a small-scatter RVE (left) and a large-scatter RVE (right) at the indicated cross-section.

values of 38 and 10 W/m K. The density and heat capacity are taken to be 1820 kg/m^3 and 120 J/kg K, respectively. The macroscopic mesh consists of 3125 four-noded quadrilaterals with four integration points (total dofs = 3276) and the micro-domain is divided into 1305 elements with the total dofs number of 1348. As mentioned in the previous example, due to constant conductivities, computation times are comparable with those of the conventional FE analysis. In Figure 6, the temperature profiles along the cross-section indicated are compared at $t = 50$ s, for small-scatter and random anisotropy. For the small-scatter case (shown left) the results following the rule of mixtures and the computational homogenization are obviously close since the microstructure is more or less homogeneous in terms of its global conductivity. However, in the large-scatter case

DOI: 10.1002/nme

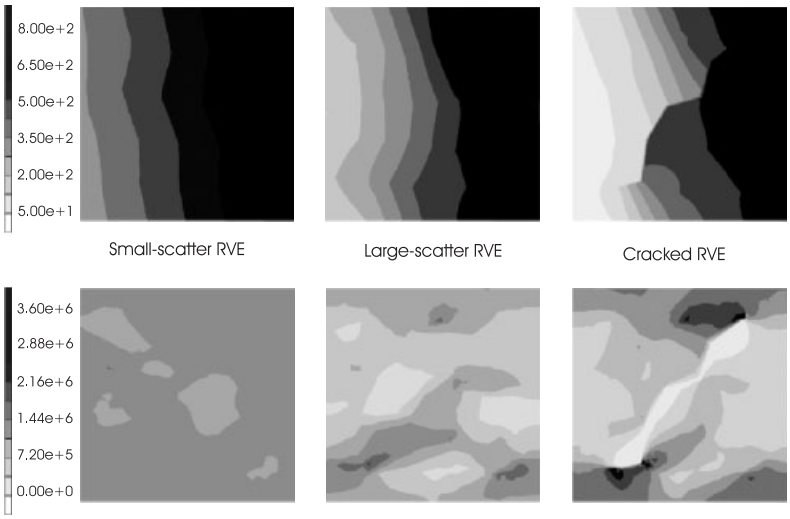

Figure 7. Comparison of the temperature fields (in °C) and the magnitude of the heat flux vector (in W/m^2) distribution at RVE level (top row, temperatures and bottom row, heat fluxes).

(shown right), the differences are pronounced; where the computational homogenization results reflect the microstructural information more adequately. For both cases, the effect of pre-damage which leads to locally reduced conductivities can clearly be observed in the temperature profiles. Evidently, the rule of mixtures cannot discriminate between these two cases which locally differ up to 100°C. In Figure 7, the distribution of the temperature and the magnitude of the heat flux at the micro level are shown for $t = 2$ s. The microstructural profiles depicted are taken at a distance of 0.3 m from the top edge of the structure on the inclined wall. Obviously, the temperature distributions become less smooth as scatter and damage are introduced in the microstructure. The crack acts as a barrier for the heat flow and therefore the heat is forced to flow over the intact narrow top and bottom regions. These microstructural phenomena are particularly important in the case of temperature-induced stress fields, as needed in thermomechanical damage predictions. The latter is an important issue in assessing thermoshock damage in refractories.

7. SUMMARY AND CONCLUSION

In this contribution, a multi-scale analysis method for the heat conduction in heterogeneous solids is presented. The approach is based on a two-level homogenization strategy, which incorporates a rigorous scale transition. The heat conduction problem is treated consistently at two distinct scales which are linked by the outlined scale bridging scheme. The macro to micro transition is achieved through the RVE boundary conditions introduced, whereas the micro to macro transition results from proper averaging relations. The macroscopic (tangent) conductivity is derived in a consistent manner. Finally, a nested finite element solution scheme is presented and implemented into a FE framework. As shown by the example problems, the method offers the possibility to include a microstructural morphology and a temperature-dependent microstructural material behavior and

DOI: 10.1002/nme

transfers the microstructural response properly to the macro level. Original aspects and the added values of the proposed approach are:

- A rigorous method for the heat conduction analysis in heterogeneous solids has been developed. The approach is particularly superior when the coupling between micro and macro scales becomes stronger, e.g. in case of a temperature-sensitive microstructural response or materials with evolving microstructure.
- Anisotropy, non-linearity and microstructure morphology can be easily introduced and investigated effectively. Particularly, temperature-dependent conductivity problems which cannot be handled by classical homogenization techniques, can easily be dealt with.
- The method offers considerable potential for thermomechanical damage predictions when combined with mechanical homogenization, with the capability to capture and quantify the interaction between thermal and mechanical fields.
- Results obtained through the proposed methodology may serve as a reference for any other simplified homogenization scheme.

The proposed method, when combined with mechanical homogenization, constitutes a powerful tool, especially at high temperatures where the material properties become strongly dependent on the temperature. The influence of microstructural evolution (e.g. damage and microcracking) on the mechanical and thermal fields and their interaction can be introduced and treated effectively. This enhances the understanding and modeling of failure phenomena and opens the possibility to identify some interesting mechanisms of failure initiation and field interaction effects which cannot be captured and described trivially without incorporating the relevant microstructural details, as done here.

REFERENCES

1. Evans AG. Microfracture from thermal expansion anisotropy—I. Single phase systems. *Acta Metallurgica* 1981; **26**:1845–1853.
2. Hashin Z. Analysis of composite materials. *Journal of Applied Mechanics* 1983; **50**:481–505.
3. Rosen BW, Hashin Z. Effective thermal expansion coefficients and specific heats of composite materials. *International Journal of Engineering Science* 1970; **8**:157–173.
4. Gibiansky LV, Torquato S. Thermal expansion of isotropic multiphase composites and polycrystals. *Journal of the Mechanics and Physics of Solids* 1997; **45**:1223–1252.
5. Noor AK, Shah RS. Effective thermoelastic and thermal properties of unidirectional fiber-reinforced composites and their sensitivity coefficients. *Composite Structures* 1993; **26**:7–23.
6. Auriault JL. Effective macroscopic description of heat conduction in periodic composites. *International Journal of Heat and Mass Transfer* 1983; **26**(6):861–869.
7. Boutin C. Microstructural influence on heat conduction. *International Journal of Heat and Mass Transfer* 1995; **38**(17):3181–3195.
8. Guedes JM, Kikuchi N. Preprocessing and postprocessing for materials based on the homogenization method with adaptive finite element methods. *Computer Methods in Applied Mechanics and Engineering* 1990; **83**:143–198.
9. Takano N, Zako M, Kubo F, Kimura K. Microstructure-based stress analysis and evaluation for porous ceramics by homogenization method with digital image-based modeling. *International Journal of Solids and Structures* 2003; **40**:1225–1242.
10. Ghosh S, Liu Y. Voronoi cell finite element model based on micropolar theory of thermoelasticity for heterogeneous materials. *International Journal for Numerical Methods in Engineering* 1995; **38**:1361–1398.
11. Jiang M, Jasiuk I, Ostoja-Starzewski M. Apparent thermal conductivity of periodic two-dimensional composites. *Computational Materials Science* 2002; **25**:329–338.
12. Ostoja-Starzewski M, Schulte J. Bounding of effective thermal conductivities of multiscale materials by essential and natural boundary conditions. *Physical Review B* 1996; **54**(1):278–285.

DOI: 10.1002/nme

13. Golanski D, Terada K, Kikuchi N. Macro and micro scale modeling of thermal residual stresses in metal matrix composite surface layers by the homogenization method. *Computational Mechanics* 1997; **19**:188–202.
14. Sigmund O, Torquato S. Design of materials with extreme thermal expansion using a three-phase topology optimization. *Journal of the Mechanics and Physics of Solids* 1997; **45**:1037–1067.
15. Smit RJM. Toughness of heterogeneous polymeric systems. A modeling approach. *Ph.D. Thesis*, Eindhoven University of Technology, 1998, http://www.mate.tue.nl/mate/publications/index.php/4/1998 [2 November 2006].
16. Smit RJM, Brekelmans WAM, Meijer HEH. Prediction of the mechanical behaviour of nonlinear heterogeneous systems by multi-level finite element modeling. *Computer Methods in Applied Mechanics and Engineering* 1998; **155**:181–192.
17. Miehe C, Schröder J, Schotte J. Computational homogenization analysis in finite plasticity. Simulation of texture development in polycrystalline materials. *Computer Methods in Applied Mechanics and Engineering* 1999; **171**:387–418.
18. Feyel F, Chaboche JL. FE^2 multiscale approach for modeling the elastoviscoplastic behaviour of long fibre SiC/Ti composite materials. *Computer Methods in Applied Mechanics and Engineering* 2000; **183**:309–330.
19. Kouznetsova VG, Brekelmans WAM, Baaijens FPT. An approach to micro–macro modeling of heterogeneous materials. *Computational Mechanics* 2001; **27**:37–48.
20. Kouznetsova VG, Geers MGD, Brekelmans WAM. Multi-scale constitutive modelling of heterogeneous materials with a gradient-enhanced computational homogenization scheme. *International Journal for Numerical Methods in Engineering* 2002; **54**:1235–1260.
21. Kouznetsova VG. Computational homogenization for the multi-scale analysis of multi-phase materials. *Ph.D. Thesis*, Eindhoven University of Technology, 2002, http://www.mate.tue.nl/mate/publications/index.php/4/2002 [2 November 2006].
22. Bigaud D, Goyheneche J-M, Hamelin P. A global-local non-linear modeling of effective thermal conductivity tensor of textile-reinforced composites. *Composites*: *Part A* 2001; **32**:1443–1453.
23. Kwon YW, Cho WM. Multilevel, micromechanical model for thermal analysis of woven-fabric composite materials. *Journal of Thermal Stresses* 1998; **21**:21–39.
24. Kwon YW. Micromechanical and thermomechanical study of a refractory fiber/matrix/coating system. *Journal of Thermal Stresses* 2005; **28**:439–453.
25. Kouznetsova VG, Geers MGD, Brekelmans WAM. Size of a representative volume element in a second-order computational homogenization framework. *International Journal of Multiscale Computational Engineering* 2004; **2**(4):575–598.
26. van der Sluis O, Schreurs PJG, Brekelmans WAM, Meijer HEH. Overall behaviour of heterogeneous elastoviscoplastic materials: effect of microstructure modelling. *Mechanics of Materials* 2000; **32**:449–462.
27. Ostoja-Starzewski M. Towards stochastic continuum thermodynamics. *Journal of Non-equilibrium Thermodynamics* 2002; **27**:335–348.
28. Gibson LJ, Ashby MF. *Cellular Solids* (2nd edn). Solid State Science Series. Cambridge University Press: Cambridge, U.K., 1997.
29. Lu TJ, Chen C. Thermal properties and fire retardance properties of cellular aluminium alloys. *Acta Materialia* 1999; **47**(5):1469–1485.

DOI: 10.1002/nme